Computers & Graphics 105 (2022) 12–24

Contents lists available at ScienceDirect

Computers & Graphics

journal homepage: www.elsevier.com/locate/cag

Special Section on VCBM 2021

Spatial-data-driven layouting for brain network visualization

Florian Ganglberger [a,*], Monika Wißmann [a], Hsiang-Yun Wu [b], Nicolas Swoboda [a], Andreas Thum [c], Wulf Haubensak [d], Katja Bühler [a]

[a] VRVis Research Center, Donau-City Straße 11-13, 1220 Vienna, Austria
[b] TU Wien, Favoritenstraße 9/11, 1040 Vienna, Austria
[c] Leipzig University, Augustusplatz 10, 04109 Leipzig, Germany
[d] Medical University of Vienna, Währinger Gürtel 18–20, 1090 Vienna, Austria

ARTICLE INFO

Article history:
Received 27 January 2022
Received in revised form 10 April 2022
Accepted 25 April 2022
Available online 29 April 2022

Keywords:
Networks
Neuroscience
Graph layouting
Brain parcellation
Anatomical layouts

ABSTRACT

Recent advances in neuro-imaging enable scientists to create brain network data that can lead to novel insights into neurocircuitry, and a better understanding of the brain's organization. These networks inherently involve a spatial component, depicting which brain regions are structurally, functionally or genetically related. Their visualization in 3D suffers from occlusion and clutter, especially with increasing number of nodes and connections, while 2D representations such as connectograms, connectivity matrices, and node-link diagrams neglect the spatio-anatomical context. Approaches to arrange 2D-graphs manually are tedious, species-dependent, and require the knowledge of domain experts.

In this paper, we present a spatial-data-driven approach for layouting 3D brain networks in 2D node-link diagrams, while maintaining their spatial organization. The produced graphs do not need manual positioning of nodes, are consistent (even for sub-graphs), and provide a perspective-dependent arrangement for orientation. Furthermore, we provide a visual design for highlighting anatomical context, including the shape of the brain, and the size of brain regions. We present in several case-studies the applicability of our approach for different neuroscience-relevant species, including the mouse, human, and *Drosophila* larvae. In a user study conducted with several domain experts, we demonstrate its relevance and validity, as well as its potential for neuroscientific publications, presentations, and education.

© 2022 The Authors. Published by Elsevier Ltd. This is an open access article under the CC BY license (http://creativecommons.org/licenses/by/4.0/).

1. Introduction

Advances in neuro-imaging have enabled big brain initiatives and consortia to create vast resources of brain data that can be mined for insights into mental processes and biological principles. This includes brain networks, representing the relations between different spatial locations in the brain of a certain modality.

In the field of network neuroscience, brain networks represent the relations between different spatial locations in the brain of a certain modality. These networks can be on various anatomical scales, ranging from brain region level [1], to even neuron-level synaptic connectivity [2], i.e., connection between neurons that can span across brain regions. The relations can be divided into anatomical/structural connectivity (anatomical links), functional connectivity (statistical functional dependencies), and effective connectivity (directed causal effects) [3]. Understanding and visualizing these networks is crucial to investigate the cognition, memory, and many neurological disorders, such as Alzheimer's disease, autism, and anxiety.

To relate brain networks to their anatomical context, anatomical data are needed. They are not a single type of data, they rather represent a diverse collection of reference templates, brain parcellations, and neuroanatomical ontologies. Together they form the common knowledge of how the brain is structured and how this structure can be referenced. A reference template is in general structural imaging data that has been combined (e.g., via image registration) to a structural representation of the brain for a group of specimens or a species. A neuroanatomical ontology is the formal representation of knowledge about the anatomy of the brain [4] of a species. This relates foremost to the composition of the brain, i.e., of which brain regions it consists and how these brain regions are subdivided (hierarchically). It may also include naming or color conventions. Brain parcellations act as links between neuroanatomical ontologies and reference templates. In principle, a brain parcellation consists of a regional annotation of every voxel in a reference template. Hence, voxels can be associated with brain regions of an ontology for visualizing anatomical context and relating voxel-level to region-level data.

* Corresponding author.
E-mail address: ganglberger@vrvis.at (F. Ganglberger).

https://doi.org/10.1016/j.cag.2022.04.014
0097-8493/© 2022 The Authors. Published by Elsevier Ltd. This is an open access article under the CC BY license (http://creativecommons.org/licenses/by/4.0/).

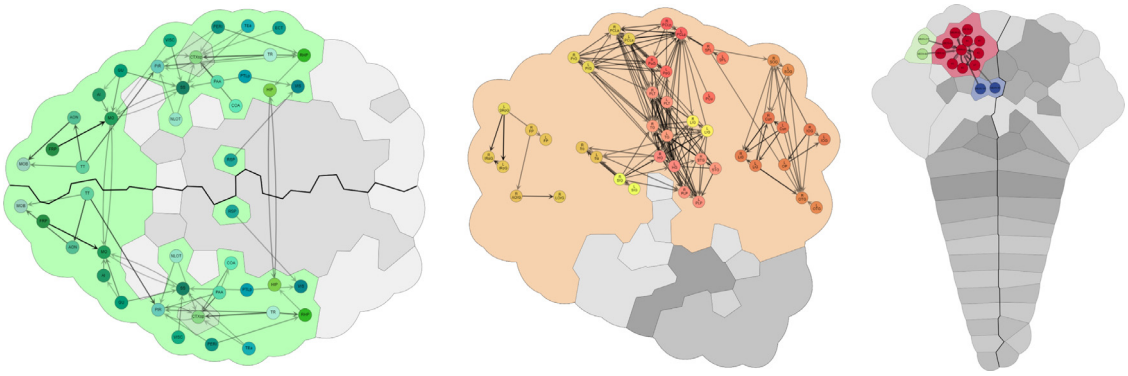

Fig. 1. *Spatial-Data-Driven Layouts* of three different brain networks of species relevant in neuroscience. Nodes represent brain regions, colored according to a common hierarchical ontology. The background parcellation colors indicate major brain regions. Gray areas represent regions without connections for anatomical context. Edge opacity shows connection strength. Left: Strongest structural connections (top 2%) within the cerebral cortex of a mouse brain, transversal view (from the top). Middle: Strongest functional connections (top 5%) within the cerebral cortex of a human brain, sagittal view (from the side). Right: Synaptic connections between exemplarily selected individual neurons (nodes) projecting from and to the mushroom body (red) in the *Drosophila* larval brain, transversal view (from the top). Neurons were assigned to brain regions (background parcellation) based on the regions they exhibit the most synapses.

Visualizations of brain networks are frequently used to show results in neuroscientific publications or for educational purpose, i.e., they are ubiquitous in literature because they quickly summarize information [5]. One possibility to visualize rich data is to use abstract visualization methods such as multidimensional scaling and scatter-plots [6]. Those methods lack anatomical context, which could provide neurobiologists with orientation, i.e., intuitively knowing where to find certain brain regions, which anatomical regions are shown, and from which area of the brain. For this purpose, a common way to visualize brain networks is a 3D node-link diagram, with brain regions rendered as spheres and connections rendered as straight lines [7,8] while occluded elements can be discovered via interactive navigation in 3D visualizations. However, navigating costs time, interactive 3D visualizations are not yet standard in electronic papers and naturally unavailable in printed media. A major issue with 2D node-link visualizations is the visual clutter that occurs when many edges and nodes overlap due to the projection of the 3D structure onto a 2D plane. Moreover, keeping an overview of the global network structure while visualizing a high level of detail becomes challenging given a finite display area, since the users can lose track of their current position while navigating.

Furthermore, most tools for such purposes are trimmed to visualize data of a particular species. For example, NeuroMap [9] visualizes the brain of the common fruit fly *Drosophila melanogaster*, where the anatomical layout of the graph was generated manually. Such an approach would be time-consuming regarding multiple species, as every species has a unique hierarchical definition of brain regions. Another problem concerning these regions is the selection regarding the level of detail within the hierarchy.

In this paper we present an approach for the visualization of 3D brain networks in 2D space that inherently preserves spatial organization and provides spatial context for orientation. Here, we use node-link diagrams as the graph visualization technique for its common usage in neuroscientific visualizations [1]. In these diagrams, we present the connectivity between brain regions, which we layout based on anatomical proximity, so that nodes that are anatomically close are also close in the graph. Furthermore, we render a brain parcellation in the background by introducing a visual design to optimize spatial orientation. Exemplary visualizations of three brains of different species can be seen in Fig. 1.

While individual parts of our approach are not novel on their own, particularly using spatial information for graph layouting [10] and providing group-level information for 2D graphs via Voronoi tessellation [11], we introduce a new concept of using these techniques for the visualization of brain networks with spatial organization. Specifically we make the following novel contributions:

- A novel method for generating *Spatial-Data-Driven Layouts* for neural networks of multiple species and perspectives. The proposed method overcomes the need of previous solutions to manually define brain region related constraints to generate *anatomically feasible layouts*.
- Visual designs providing a consistent spatial context to the user to ease orientation and visual comparison of different brain networks.
- A qualitative study that shows that *Spatial-Data-Driven Layouts* allow neuroscientists a faster overall understanding of 2D network graphs compared to traditional brain network visualization techniques.

2. Related work

In recent years, an abundance of toolboxes have been published [12–14] that offer computation and visualization of multimodal connectivity data. While they provide a rich set of statistical and mathematical methods, their visualizations are static, and they often require experience in Matlab or Python scripting. In contrast, visualization methods support the processing of complex information, so neuroscientists can focus on understanding the data rather than handling it. This section gives an overview on visualization tools for connectivity data targeting a 3D anatomical context with respect to our method.

A common way to visualize brain networks in neuroscientific publications are 3D node-link diagrams [15–17]. In these diagrams, network connections (edges) are often rendered as straight lines or arrows between spheres representing brain regions (nodes) across a 3D anatomical representation of the brain to help neuroscientists to orient themselves. One example is used in BrainNet Viewer [8], a graph-theoretical network visualization toolbox to illustrate macro-scale human brain networks as ball-and-stick models. It displays combinations of the brain surface, nodes, and edges from multiple perspectives (sagittal, axial or coronal) and allows the user to adjust display properties like color and size of the network elements. Although this approach is intuitively understandable, visual clutter increases with the amount of edges and nodes due to the linear projection from 3D to 2D. With our method, we overcome this problem by adapting the graph layout based on spatial relations.

Node-link diagrams are also used by the Connectome Visualization Utility [18], which offers a matrix (heatmap) and a

circular representation [19] of the network in separate views that are linked with each other. To counteract visual clutter, these views offer a selection/highlighting of nodes and edges, so one can focus on specific parts of complex networks. Bezgin et al. [20] also employed user-selected nodes to visualize only relevant sub-networks in the Macaque monkey brain. In this case, brain regions from a hierarchical ontology can be chosen to define which connections should be shown as arrows overlaying 3D brain anatomy, i.e., a 3D node-link diagram without depicting the nodes. Another example is BrainTrawler [7], a task-driven, web-based framework that incorporates visual analytics methods to explore heterogeneous neurobiological data, including their spatial context. It enables neuroscientists to analyze of the genetic and functional characteristics of brain networks in real-time via linked 2D-slice views and 3D network visualizations, as well as a visual-query based interaction scheme for exploring sub-graphs. Similar approaches using query-guided interactions for exploring electron microscopy stacks has been proposed by Beyer et al. [21, 22] in the ConnectomeExplorer. Here, labeled neuronal connections can be queried, and visually explored in linked views. These views comprise a 3D volume/mesh rendering, a 2D slice view, connectivity graphs, a tree-view showing the hierarchical structure of segmentations, and several statistical views (histograms, scatterplots etc.). All these interactive 3D network visualizations with linked views [7,19–21] contribute spatial context and enable the user to focus on relevant sub-networks. Nevertheless, navigating these approaches cost time, require domain expertise, and are naturally unavailable for printed scientific papers. This is not an issue with our method, since its output is a static figure with inherent spatial information.

Although the 3D spatial representation of networks provides anatomical context, 2D node-link diagrams with flexible layouts are better suited for comparing connectivity [23] or identifying modules (well-connected groups of nodes) [24]. For this reason, BrainModulizer [25] uses a linked presentation of anatomy in 3D, and 2D networks to enable neuroscientists to interactively explore functional connectivity. Spatial correspondence is indicated via color coding of hierarchically organized brain modules, but can be also established via brushing/selecting nodes in one of the views. Analogous to BrainModulizer, BRAINtrinsic [26,27] aimed to explore brain connectivity with node-link diagrams based on network topology. Instead of arranging nodes, they mapped the network to a topological space by taking the networks intrinsic geometry into account. For this purpose, they performed dimensionality reduction (multidimensional scaling, isomap, and t-distributed stochastic neighbor embedding) on structural and functional connectivity data. In a 3D view that shows the network as a node-link diagram, one can interactively switch between anatomical and topological spaces, show/hide particular brain regions and compute network measures. This approach has been taken further in the NeuroCave visualization system [28], optimized for virtual reality environments. Networks are shown in a coordinated view, so the network is visible in both a 3D anatomical space and a topological space simultaneously. These approaches combine the advantage of 3D spatial representations with the flexibility of 2D node-link diagram layouts. However, the spatial context needed for the 2D node-link diagram is provided via interaction with a linked view, which is again not available for printed scientific papers, and not yet standard for their electronic versions. With *Spatial-Data-Driven Layouts* this can be avoided, since spatial context is not only an intrinsic part of the visualization, but also of the graph layout.

Spatial relations and anatomical meaning can be integrated into an abstract visualization directly while avoiding occlusions and clutter simultaneously. For example, Jianu et al. [29] used planar projections of fiber tracts generated by Diffusion Tensor Imaging to visualize neuronal connectivity as bundles, where single bundles can be highlighted for visual distinction. The endpoints of these bundles project directly onto a silhouette of the brain, providing spatial orientation. Due to a lack of labels and annotations, it is not possible to identify individual brain regions. An abstract visualization was proposed by McGraw et al. [30], who positioned the nodes of a graph using the automated anatomical labeling (AAL) brain atlas, discarding one of the three coordinates. The nodes are grouped by the hemisphere (left, right) and their corresponding brain lobes. Minimizing the overlap is achieved by using the method by Misue et al. [31]. The color of the nodes is determined by the lobe it belongs to, while the radius is proportional to the number of incident edges of the node. Edges are filtered and bundled in a similar approach as described by Holten and Van Wijk [32]. Visualization of inter- and intrahemispheric connectivity is separated to reduce clutter in interhemispheric connectivity. Another approach that uses edge bundling was introduced by Böttger et al. [33] who bundled edges within a brain parcellation to visualize groups of functional connections between brain areas. While edge bundling reduces visual clutter caused by edges, they do not reduce the clutter caused by overlapping nodes caused by 3D to 2D projections. Our *Spatial-Data-Driven Layouts* use force-directed layouting to avoid overlapping nodes, while edge cluttering is reduced by using edge routing.

As an alternative to visualize the anatomical context in addition to node-link diagrams, the context can be also integrated directly into the graph layout. What are known as "anatomical layouts" are abstract 2D representations of brain regions, i.e., the 3D brain anatomy is flatted to a 2D space. NeuroMap [9] renders an interactive two-dimensional graph of the fruit fly's brain and its interconnections in the form of a circuit-style wiring diagram. Anatomical context is provided by partitioning the canvas into compartments that form an abstract representation of actual brain regions. For this purpose, fixed compartment positions that have been manually defined in collaboration with neuroscientists are used to depict the overall structure of the brain. The visualization can be interactively adapted by adding new connections from additional data, filtering, highlighting, or layout adjustments. A similar, static, visualization approach has been used by Caat et al. [11] and Ji et al. [34], which maps functional networks derived from electroencephalography (EEG) to a planar projection of the human skull. To avoid cluttering, only the coherence between functional units, i.e., network modules, units are shown in a single image. The corresponding functional units of the EEG electrodes are indicated by colored Voronoi tessellation in the background. The downside of these approaches [9,11] is the manual labor that is required to create these layouts. Hence, they are inherently time-consuming regarding multiple species, as every species has a unique hierarchical definition of brain regions. We overcome this limitation by proposing a data-driven approach.

3. Requirements

Based on a long-term collaboration with neuroscientists working on neural networks from humans, mice and *drosophila melanogaster*, we identified the following requirements for a method to generate *Spatial-Data-Driven Layouts* of brain networks:

(R1) Anatomically Feasible *The graph layout should intrinsically preserve the spatial organization of the network, i.e., nodes related to brain regions that are anatomically adjacent remain close in the graph layout. The layouting should also deliver stable, anatomically feasible, layouts for partial networks, i.e., networks spanning only a part of the brain, to facilitate comparability of these networks.*

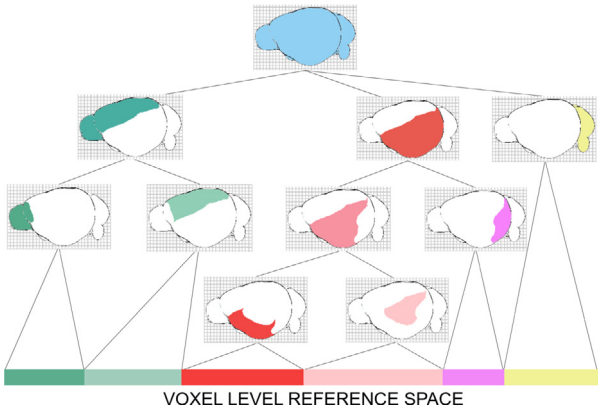

Fig. 2. Scheme of a *Hierarchical Representation of Brain Regions* of a mouse brain. The lowest level represents a voxel-level reference space, while higher levels comprise brain regions.

- **(R2) Data Driven** *The vast number of connections and brain parcellations, i.e., different regions, within the brain makes manual arrangement of data an extensive task. Therefore, the method should be able to handle the layouting in a data-driven way, i.e., without manually defined spatial restrictions on the positioning of nodes.*
- **(R3) Species-Independent** *Each species has a unique brain anatomy and parcellation, so the method should work independently of these differences.*
- **(R4) Perspective-Independent** *Different perspectives, e.g., transversal (from the top) and sagittal (from the side) should be possible to provide orientation, i.e., representing the perspective shape of the brain.*
- **(R5) Providing Anatomical Context** *The final visualization should provide sufficient context to facilitate the anatomical localization of a brain network.*
- **(R6) Adaptable with regards to Anatomical Detail** *It should be possible to highlight the anatomical detail of the graph according to information density, (i.e., show more anatomical detail for highly connected regions, or where networks with more than one node per region exceeding the resolution of the hierarchical parcellation), or by the region's anatomical size, i.e., where anatomical detail is evenly distributed over regions with equal size.*
- **(R7) Consistent in Spatial Organization with respect to Changes** *The layouting should be stable concerning changes in the selection of visualized network nodes and brain regions, and therefore, the mental map of the neuroscientist be retained.*
- **(R8) Overlap-efficient** *Overlap of nodes and edges should be minimized.*

4. Methodology

When using graph layouting algorithms, spatial structures and orientation get lost if such information is not represented in the graph data. We utilize this presumed problem by proposing a multi-stage algorithm, which facilitates connectivity describing anatomical proximity of each brain region (*Parcellation-derived Connectivity*) for graph layouting, and the actual connectivity of interest for visualization (*Rendered Connectivity*). This means that anatomical adjacency of regions and overall shape of the brain is reflected in the layout.

4.1. Input data

Hierarchical Brain Parcellation: This data represent the overall information of the species-specific hierarchical parcellation of the brain. This parcellation hierarchically subdivides a 3D reference space into brain regions, where each brain region is defined via 3D coordinates. These can be either the regions' voxel-level representations on the space, or, if not available, the brain regions' centers of mass (however the center is defined). Furthermore, for each region it includes a name, an acronym, a color-code, the region's size, and a list of its sub-regions. This data can be typically derived from brain reference atlases such as the *Allen Mouse Brain Common Coordinate Framework* [36], the *Allen Human Reference Atlas,Ding2016*, and the larvalbrain platform [37]. A scheme of the *Hierarchical Representation of Brain Regions* consisting of the higher hierarchy levels of the *Allen Mouse Brain Common Coordinate Framework* can be seen in Fig. 2.

Brain Network: A brain network of interest is given as graph of nodes encoding neural elements at brain region level, and edges with weights indicating and characterizing the connectivity between these nodes, for example, functional resting-state connectivity from the *Human Connectome Project* [38] or structural connectivity from the Allen Mouse Brain Connectivity Atlas [39] (see mouse and human usage scenarios in Sections 5.1 and 5.2). In case of availability of more fine grained connectivity information there can be more than one node related to a brain region, for example, neuron-to-neuron synaptic connectivity data from CATMAID [40] (see Drosophila usage scenario in Section 5.3).

4.2. Approach

The algorithm for *Spatial-Data-Driven Layouts* consists of seven principal steps, depicted in Fig. 3. In principle, the nodes of a brain network are projected onto a 2D plane, depending on the desired perspective. In case the brain network does not cover the whole brain, additional nodes are added to represent the missing anatomical context (Step 1, 2, 3). Then, force-directed layouting based on *Parcellation-derived Connectivity* is used to adapt the initial 2D node projection so that nodes that are spatially close in the anatomical reference space are also close in the 2D graph (Step 4). To enforce an even distribution of nodes, another force-directed layouting step based on Delaunay-triangulation is performed (Step 5). In the background of the graph, a colored Voronoi tessellation is added to represent anatomy and overall shape (Step 6). Finally, the original brain network's edges are rendered. (Step 7).

Step 1 - Preprocessing: For producing anatomically feasible layouts (**R1**) in a data driven way (**R2**), we introduce a *Parcellation-Derived Connectivity* (Fig. 3 (1)) that represents the closeness of brain regions in the anatomical reference space. We derived this measure from the parcellation of brain regions on a 3D reference space by computing the number of neighboring voxels (6-connectivity) between brain regions across all hierarchy levels. We normalize the measure by the total number of voxels of the respective two brain regions, otherwise the measure would directly depend on the size of the regions. The localized nature of this connectivity (only neighboring brain regions are connected) enables graph layouts that retain these local structural relationships between brain regions. Alternatively, or in case no parcellation is available, it is also possible to approximate this measure with the reciprocal distance between region centers (however this center is defined), which leads to inferior results. For details of the effect on the layout see Section 5. If more than one node per brain region is included, i.e., the original network is more fine grained than the given *Hierarchical Brain Parcellation*, we add additional edges with the maximum weight between to represent their anatomical closeness.

Step 2 - Graph Completion: Brain networks are generally anatomically incomplete, i.e., not covering the whole brain. Thus, to

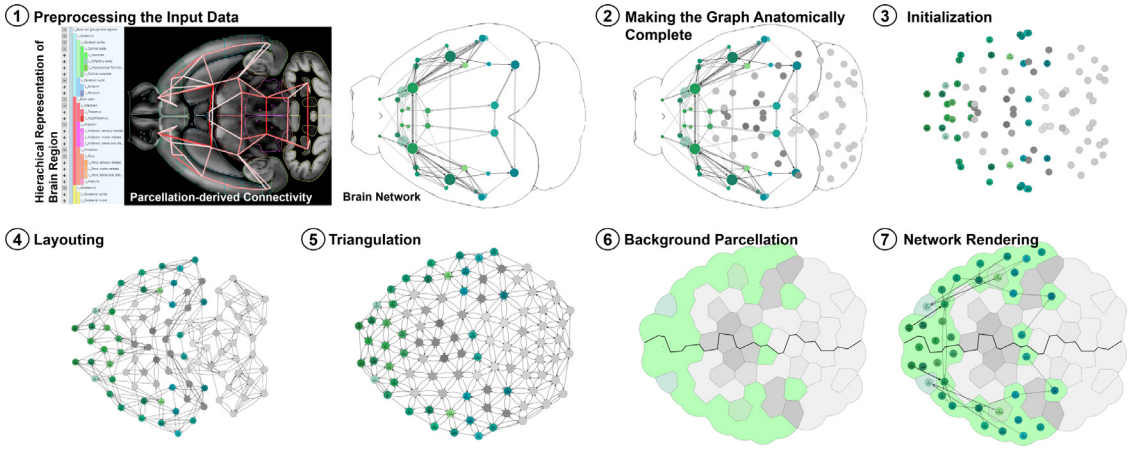

Fig. 3. Principal steps to generate spatial-data-driven layouts. **(Step 1) Preprocessing the Input Data** Preprocessing a *Hierarchical Representation of Brain Regions* to generate *Parcellation-derived Connectivity* which will be used in later steps to layout a brain network. **(Step 2) Making the Graph Anatomically Complete:** If the brain network does not cover the whole brain, the missing anatomical context is added as *Shadow Nodes*, covering brain regions not being part of the original brain network (gray). **(Step 3) Initialization:** Projecting the 3D positions of the brain network regions as nodes on a canvas, depending on the desired perspective (here: transversal view). **(Step 4) Layouting:** Layouting the graph based on the *Parcellation-derived Connectivity* using a force-directed layouting algorithm. **(Step 5) Triangulation:** To evenly distribute the nodes, Delaunay-triangulation between the nodes is performed. This triangulation is used as edges to perform another force-directed layouting with the results of the previous step as initialization. **(Step 6) Background Parcellation:** Parcellating the background for anatomical context and providing an overall shape. A Voronoi tessellation is used, where cells that belong to the same brain regions are grouped together [35]. **(Step 7) Network Rendering:** Rendering the nodes and edges of the brain network (*Rendered Connectivity*).

include the missing anatomical context (**R1, R5, R7**) into our layouting and the final graph representation, we add *"Shadow Nodes"* covering the parts of the brain not being part in the original network (Fig. 3 (3)). These additional nodes will be used only for layouting process, but are not rendered. As a consequence, they fill space in the graph layout, but are otherwise invisible. This empty, used-up space represents the missing anatomical context, where the presence of these nodes is only indicated by a gray background coloring (hence the name *"Shadow Nodes"*). In Fig. 3 (Steps 2,3,4, and 5) these nodes are shown in gray to help understanding the method.

The selection of the hierarchy level of the parcellation used for the *Shadow Nodes* is one of the degrees of freedom influencing the layout and the final visual appearance of the background. Depending on how much context is desired, the *Shadow Node Ratio* (the area that the rest of the brain will take for the layouting and background coloring in relation to the brain network nodes – see *Step 6 – Background Parcellation*) can be adapted:

- *Shadow Node Ratio* = 0: only brain network nodes will be layouted and used for background coloring
- *Shadow Node Ratio* = 1: The hierarchy level for the background context will set to a level, where the *Shadow Nodes*, i.e., the rest of the brain, will cover the same area (on the 2D canvas) as brain network nodes.
- *Shadow Node Ratio* = N: The hierarchy level for the background context will set to a level, where the *Shadow Nodes*, i.e., the rest of the brain, will cover N-times the area (on the 2D canvas) as brain network nodes.

The effect of this parameter can be seen in Fig. 5. As a consequence, the overall shape of the visualization is still preserved even for sub-networks that do not cover the whole brain (**R5, R6**).

Since the hierarchical parcellation is not balanced by the brain region's anatomical size, it is not possible to choose a hierarchy level that results in a number of *Shadow Nodes* that fit the *Shadow Node Ratio*. Therefore, the hierarchy is traversed based on region size, so that every *Shadow Nodes* covers an equal anatomical space/region size.

Step 3 - Initialization:

If layouting (Section 4.2, *Step 4 - Layouting*) would be performed with random initial position of the nodes on a 2D canvas, its resulting representation would still resemble the anatomy due to the construction of the graph in *Step 1 - Initialization* and *Step 2 - Graph Completion* of our method. Hence, a random initialization would lead to tilted, turned, and deformed compared to common standard views aligned to the main axes of the brain.

In informal interviews, domain experts expressed that the orientation is crucial for the acceptance of the visualization. Otherwise, they could not sufficiently grasp the spatial structure after initially looking at the graph (**R4**).

Here, sagittal (from the side) and transversal (from the top) are typical views used in neuroscience and provide neuroscientists with an initial orientation. We approximate these views by choosing projection planes aligned to the respective main axes of the brain as initialization for layouting.

Based on the user's desired orientation of the final graph, we select a plane (e.g., X-Y plane or Y-Z plane) and orthogonally project the 3D positions of the brain network nodes on it to define the initial node positions for the layouting (Fig. 3 (2)). For the sagittal view, where, due to the brain's symmetry, the left and right versions of brain regions would directly overlap, we performed the layouting only on one side, and positioned the nodes of the respective other side's brain regions at a tilted displacement. This mimics a form of perspective distortion, and enables the viewer to always find the left/right versions of a brain region at the same distance and angle from each other.

Step 4 - Layouting: We layout the graph based on the *Parcellation-derived Connectivity* computed in *Step 1 - Preprocessing* using a force-directed layouting algorithm to realize **R1, R2**, **R7** and **R8**. Here we used CoSE-Bilkent [41]. Depending on the occlusion/overlap of nodes in *Step 3 - Initialization*, the forces applied by the layouting algorithm need to be manually adjusted. Which forces these are, depends on the chosen algorithm. For CoSE-Bilkent this is further discussed in Section 4.3. The effect of parameter adjustment is demonstrated in *Supplementary Video 1*. In the transversal view for the mouse brain, weak forces are enough due to the flatter composition of the regions (Fig. 3 (4)).

Parameters for the sagittal view require stronger values, to pull regions adjacent to each other together and push distant regions further apart.

Step 5 - Triangulation: Although the previous step will minimize node overlap, it is not guaranteed to lead to no overlap at all. To counteract this, we want to drive the layout towards an even node distribution, i.e., nodes being equidistant to each other. Therefore, we generate edges based on a triangulation between the nodes (Fig. 3 (5)) (**R8**) and perform a force-directed layouting again.

Step 6 - Background Parcellation: We are parceling and coloring the background to generate anatomical context (**R5**).

First, all 2D nodes (real network nodes and shadow nodes) on the 2D canvas are parceled via a Voronoi tessellation. Naturally, the Voronoi tessellation would parcel the whole rectangular canvas. To limit the tessellation to an area that resembles anatomy, i.e., around the nodes, we draw a convex hull with a certain padding around the nodes. Along this hull, we place virtual nodes that will be only considered by the Voronoi tessellation. By setting the cells of these virtual nodes to invisible, the remaining cells of the network and shadow nodes form the desired shape (Fig. 3 (6)). Then, we group the cells together based on background regions. To identify these background regions, a recursive algorithm is used, that, given a user-defined *Number of Background Regions* as parameter, traverses the hierarchy up to find either brain regions higher in the hierarchy with similar anatomical size or similar number of edges. Therefore, the background can be either focus on anatomy (size of brain regions), or provide context based on the information content (number of edges) (**R6**).

To support the perception of orientation of the domain experts with respect to the network of interest, we color the cells of the parcellation by their associated brain regions' colors which enables the user their identification. Fig. 4 shows this approach with different *Numbers of Background Regions* based on the region size. Background regions are further indicated by an outline around the groups/background regions in the background (Fig. 3 (6)). Note that in Fig. 4, 5 and 6, we colored the whole background (even the *Shadow Nodes*) to demonstrate the process of background drawing. Otherwise, the background of regions that do not have connections, i.e., are not part of the network (*Shadow Nodes*), are colored in gray to not catch the viewer's focus.

To provide further orientation for the transversal view, we use the circumstance that the brain is typically divided into two hemispheres. Here, we highlight borders between cells of the left and right hemispheres in bold black, which leads to a middle line separating these two parts of the brain.

Step 7 - Network Rendering: Drawing the brain network (Fig. 3 (7)). Here, we label network nodes at region level with the region's name, including its brain hemisphere (L as prefix for left or R as prefix for right) to add anatomical context at network level (**R5**). Here we use common acronyms often included in brain ontologies, as the full name would not fit into the node. The color coding is derived from brain reference atlases [36,42], where every brain structure is assigned a distinct color based on its hierarchical level in the brain ontology. For brain networks whose resolution exceeds the *Hierarchical Brain Parcellation*, i.e., the network's brain regions are more fine grained than the parcellation, multiple nodes per brain regions are added with similar coloring and rendered adjacent.

The opacity of rendered edges/links is representing the connectivity strength (e.g., structural, functional or genetic) between nodes, causing weak connections to appear more transparent. Note that due to clutter, we only render the strongest connections in the figures of in this paper. Hence, some nodes that are part of the networks, i.e., they have connections, are rendered without

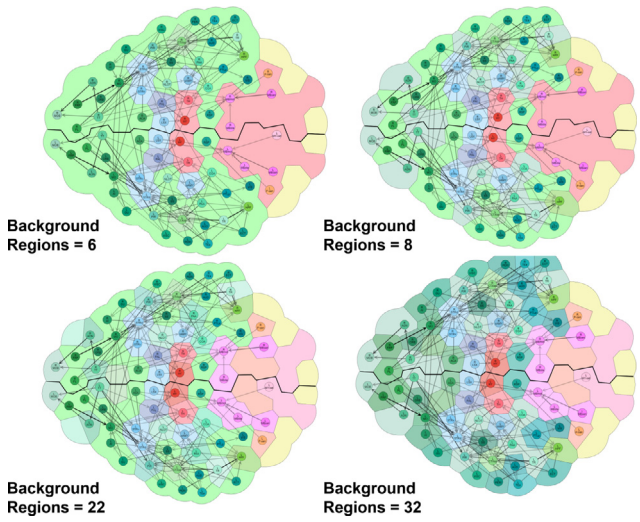

Fig. 4. Effect of different *Number of Background Regions* on the context visualized in the background of the brain network (strongest structural connections in the whole brain), as described in Section 4.2, *Step 6 - Background Parcellation*. A background region is represented as parcels with similar color and enclosed by an outline.

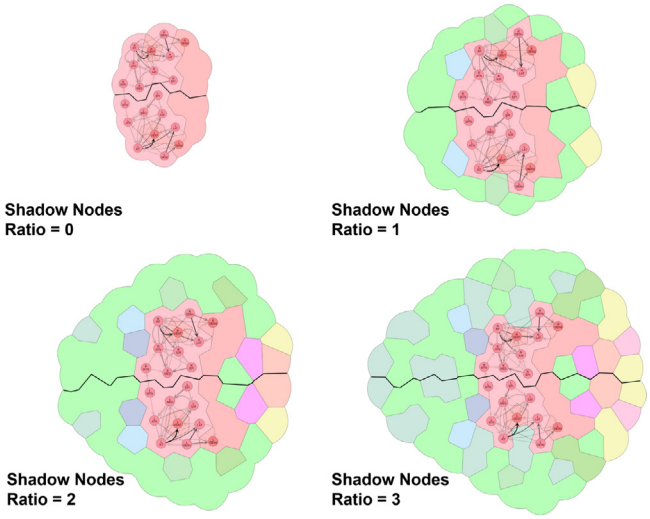

Fig. 5. Effect of a different *Shadow Node Ratios* on the context visualized in the background of brain network (structural connectivity within the thalamus), as described in Section 4.2, *Step 2 - Making the Graph Anatomically Complete*.

edges. Other alternatives, such as thickness or coloring causes more clutter, especially with growing number of edges. Edge bundling or different edge layouts (**R8**) can be used to further reduce this, several of them (orthogonal and organic edge layouting) are shown in the user study (see Fig. 11 and Supplementary Material).

4.3. Implementation

We used the graph-drawing library Cytoscape.js [43] for the implementation of a interactive visualization. Here, we selected the CoSE-Bilkent algorithm [41] for layouting in *Step 4 - Layouting* of our method for its speed and usability. There is no limitation to use different force-directed algorithms. CoSE-Bilkent represents merely one approach to show that force-directed layouts can be used for *Spatial-Data-Driven Layouts*.

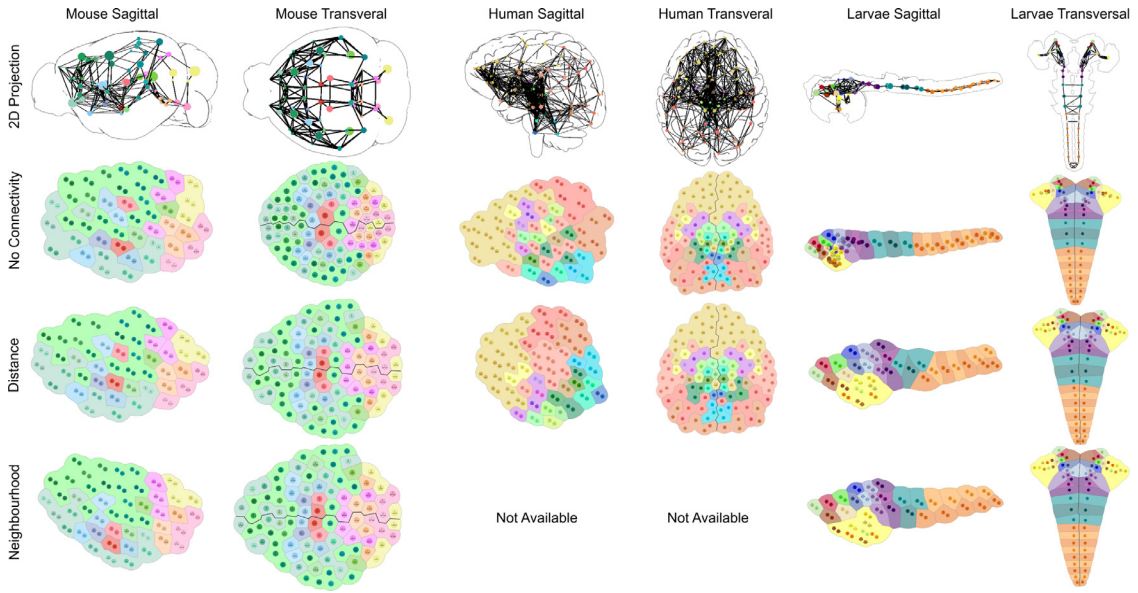

Fig. 6. Effects of *Parcellation-derived Connectivity* on the *Spatial-Data-Driven Layouts* of different species and views. Columns show species (mouse, human, and *Drosophila* larvae) and view (sagittal and transversal), rows the 2D projection of *Parcellation-derived Connectivity* (*2D Projection*), layouting of the nodes without connectivity at all, i.e., without *Step 4 - Layouting* of the approach (*No Connectivity*), layouting with the reciprocal distance between brain regions as *Parcellation-derived Connectivity* (*Distance*), and layouting using the number of neighboring voxels (6-connectivity) between brain regions as *Parcellation-derived Connectivity* (*Neighborhood*). There was no voxel-level definition of brain regions matching the *Hierarchical Representation of Brain Regions* available for human, hence the layouting is missing in the last row. Edges for the 2D projections represent the neighborhood-based *Parcellation-derived Connectivity* for mouse and *Drosophila* larvae, and distance-based for human.

For our implementation, we omitted the nested layouting/compound layouting functionality of CoSE-Bilkent, since it produced rectangular compartments which interfered with the shape/outline of the layouted graph. We investigated the effect of the algorithm's parameters, and selected three (node repulsion, edge length and edge elasticity) that had the strongest effect on the layouting. While node repulsion acts as pushing force between nodes, edge length and edge elasticity controls how nodes are pulled together based on *Parcellation-derived Connectivity*. We created a prototype of an interactive visualization, where these parameters can be iteratively adapted via sliders in real-time, so that one can find a trade-off between mapping spatially close nodes in the anatomical reference space to spatially close positions in the 2D graph, and keeping the overall shape of the brain. An example of how the layout is reacting to parameter changes can be seen in *Supplementary Video 1* for full and partial networks.

5. Usage scenarios

We created usage scenarios on three different species (mouse, human and *Drosophila*) relevant for neuroscience to showcase anatomical feasibility (**R1**) of our approach, its general applicability on different brain architectures (**R2, R3**) and for different perspectives (**R4**). The effectiveness of our proposed visualization on the perception of brain networks by neuroscientists was evaluated in a separate user study in Section 6.

For each brain architecture, we created *Spatial-Data-Driven Layouts* depicting common views in neuroscience (sagittal and transversal) and different ways to create *Parcellation-derived Connectivity*, i.e., distance or neighborhood based (**R2, R3, R4**). To qualitatively evaluate the anatomical feasibility of the generated layouts (**R1**), we produced visualizations that re-imagine figures from neuroscientific publications to show that our approach can be used to present this information in a similar way. We omitted a numeric, quantitative evaluation based on the distance of spatially-close nodes in the 2D graph. Here, one would evaluate the closeness of nodes in the resulting 2D graphs by their spatial closeness in 3D, which already depends on the input of the force-directed layout algorithm and the spatial closeness in 3D (*Parcellation-derived Connectivity*), hence one would evaluate the force-directed layouting algorithm, and not our approach.

5.1. Mouse brain

Setup: The mouse brain is a model organism widely used in studies about brain connectivity [16,39,44]. To provide a common ontology and reference space, the *Allen Institute* released a common coordinate framework on a cellular level resolution for analysis, visualization, and integration of multimodal and multiscale datasets [36]. It does not only have a voxel-level representation of brain regions, but also a brain region ontology, i.e., a *Hierarchical Representation of Brain Regions*. We used this data to create two types of *Parcellation-derived Connectivity*: The number of neighboring voxels (6-connectivity) between brain regions (shown as edges in Fig. 6, *2D projection*), and the reciprocal distance between their center-of-gravity.

The effects of using these connectivities on the *Spatial-Data-Driven Layouts* can be seen in Fig. 6. Here, we distinguish between the sagittal and transversal view. As one can see in Fig. 6, *2D projection*, the mouse brain is rather flat in the transversal view, with rather few brain regions occluding others, in contrast to the sagittal view. Therefore, for the transversal projection, the effect on the spatial-data-driven layouting is limited. The effect increases with the size of the network, as can be seen in the distribution of 997 brain regions/nodes in Fig. 8.

Results: To verify if *Spatial-Data-Driven Layouts* can be used to produce figures for neuroscientific publications, we re-imagined an artistically drawn brain network suggested by our domain experts. Fig. 7 shows the brain reward circuitry in the mouse brain as depicted by Russo et al. Fig. 1 [45]. For this figure, we use structural connectivity [39] to create a brain network between brain regions that correspond to the ones given in the paper [45]. Note, that the structural connectivity and the dopaminergic circuitry

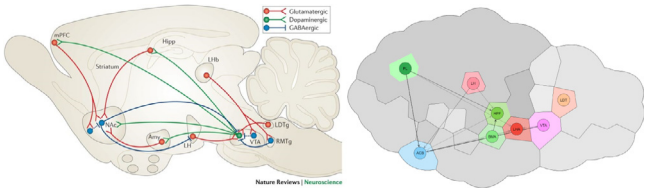

Fig. 7. Schematic of brain reward circuitry in a mouse brain as depicted by Russo et al. Fig. 1 [45], with and without colored context. The regions in the paper figure correspond in the following way (paper figures' region = this figures' regions as node labels): mPFC/medial prefrontal cortex = PL/prelimbic area, NAc/nuclues accumbens = ACB/nucleus accumbens, Amy/amygdala = BMA/basomedial amygdalar nucleus, Hipp/hippocampus = HPF/hippocampal formation, LHb/lateral habenula = LH/lateral habenula, LHA/lateral hypothalamus, VTA/ventral tegmental area, and LDT/laterodorsal tegmental nucleus.

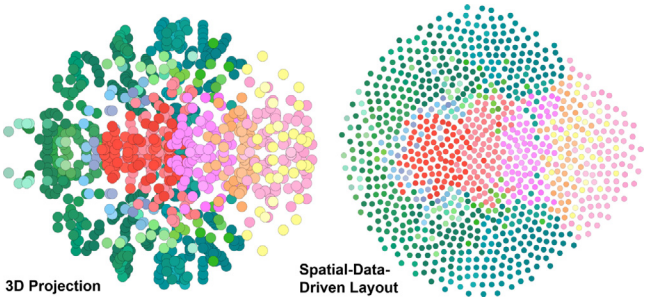

Fig. 8. Effect of *Spatial-Data-Driven* layouting on node distribution for larger networks (997 nodes). The left side shows a transversal 2D projection, the right side a *Spatial-Data-Driven* layout of the same network. Background, labels and edges are removed for the clarity of the layout.

do not represent the same modality, hence, it can only be seen as an approximation, and as a consequence, not all connections are similar or present. We investigated then if the brain regions are correctly adjoining with the *Interactive Atlas Viewer* [46]. The only obvious inconsistency was the distance between the lateral habenula (light red, LH) and lateral hypothalamus (red, LHA), whose parent regions (thalamus and hypothalamus) are positioned next to each other. Closer inspection revealed, that the LH lies at the superior part of the thalamus, while the LHA lies at the lateral part of the hypothalamus. Hence, both regions are not adjoined, and are indeed positioned correctly. The visual appeal of this diagram was then tested in a user study, which can be found in Section 6.

5.2. Human brain

Setup: Similar to the mouse brain, the *Allen Institute* released a reference atlas, the *Allen Human Reference Atlas* [42], to provide a common reference space for the human brain. In contrast to the mouse brain, the atlas provides only high-resolution histology 2D slices, not a common coordinate framework to derive the voxel-level representation of brain regions. Therefore, neighborhood-based *Parcellation-derived Connectivity* could not be evaluated in this scenario. We use data from a paper previously published by Hawrylycz et al. [47], which provided 3D positions of samples labeled with *Allen Human Reference Atlas* brain regions to create the brain regions' reciprocal distance between them (edges in Fig. 6, *2D projection*). Note, that there have been recent releases of voxel-level common coordinate frameworks with region-level annotations [48,49] that would be also suitable for applications in the future.

We visualized the effects of using these connectivities on the *Spatial-Data-Driven Layouts* similar to the usage scenario in

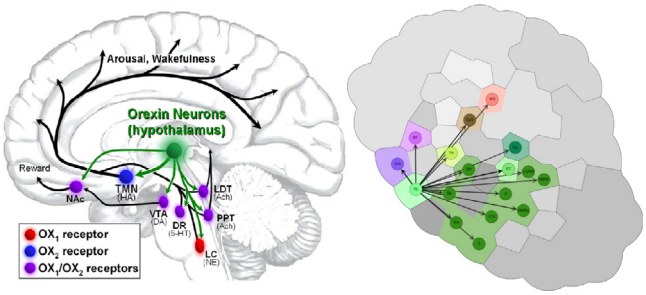

Fig. 9. Orexinergic neuron projections originating from the hypothalamus in the human brain. Brain region hierarchy level was selected to cover the majority of brain regions depicted by Gotter et al. Fig. 6, green [50]. Strongest 20% of outgoing functional resting-state connections of the hypothalamus.

the mouse brain (Fig. 6). Similarly, the transversal view already showed promising results when layouting without connectivity (Fig. 6, *No Connectivity*), mainly because of the human cortex's parcellation in frontal, lateral and posterior lobes.

Results: Again, we re-imagined an artistically drawn brain network suggested by domain experts to showcase the applicability of *Spatial-Data-Driven Layouts* for neuroscience publications. Gotter et al. (Fig. 6, green) [50] published a figure showing orexinergic neuron projections originating from the hypothalamus in the human brain. We sought to reproduces the information shown by Gotter et al. with our *Spatial-Data-Driven Layouts* by visualizing the strongest outgoing connections (top 20%) from the hypothalamus on a hierarchical brain region level covering the majority of the paper's brain regions (Fig. 9). Since no structural connectivity was available, we substituted functional resting-state connectivity from the *Human Connectome Project* [38]. This led to a surprisingly accurate overlap of the papers circuit according to our domain experts: The VTA/ventral tegmental area, ACB/nucleus accumbens (equals NAc/nucleus accumbens), MBRa/midbrain raphe nuclei (covering DR/dorsal raphe nucleus), and the MBRF/midbrain reticular formation (covering PPT/pedunculopontine tegmental nucleus) are among the strongest connections. LDT/lateral dorsal tegmental nucleus and LC/locus ceruleus were not covered in the data by Hawrylycz et al. [47], but their parent region PTg/pontine tegmentum (including 20 other subregions) was still within the strongest 40% of the connections (not shown in figure). Closer inspection of the brain regions' positions with the *Interactive Atlas Viewer* [46] revealed consistency with brain anatomy. Obvious dislocations, like the split within brown regions (limbic lobe) can be attributed to the distance-based *Parcellation-Derived Connectivity*. Although they are adjoined, their centers of gravity are farther apart due to their anatomical structure. Neighborhood-derived connectivity has the potential to compensate this issue, as can be seen in the mouse usage scenario. Visual appeal of this figure was again tested in the user study (Section 6).

5.3. Drosophila larval brain

Setup: The neural circuits of the common fruit fly *Drosophila melanogaster* are studied to investigate the generation of complex behavior. Especially their larval stages are examined [51], where their brains are with 10,000–15,000 neurons still small and compact, and therefore less complex. Visualizations of individual neurons and neuronal circuits are subject to current research [2], but their representations in relation to anatomical context require manual definition and annotations [9]. To solve this problem with *Spatial-Data-Driven Layouts*, we took a hierarchical definition of compartments/brain regions used in

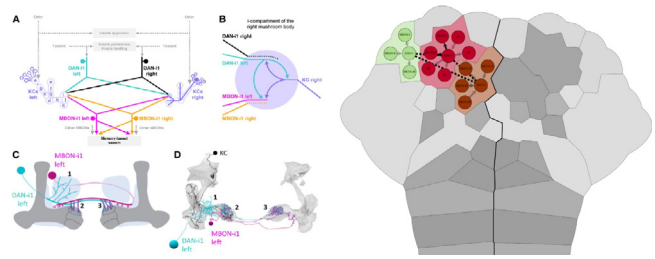

Fig. 10. DAN-KC-MBON circuitry as published by Schleyer et al. [53] (Fig. 2) in the mushroom body (red), inferior protocerebrum (brown), and superior lateral protocerebrum (green). Solid arrows represent synapse counts between the neurons (nodes), dashed lines between DAN-i1 neuron nodes (in multiple regions) indicate that it is actually the same neuron present in these three regions.

the *Drosophila* community [52], and created neighborhood-based (edges in Fig. 6, *2D projection*), and reciprocal distance-based *Parcellation-Derived Connectivity* similarly to the mouse usage scenario. As research on the *Drosophila* brain focuses on individual neuronal circuits rather than brain regions (e.g., Saumweber et al. [51]), we sought to adapt the region-level visualization we used in the mouse and human usage scenario with neuron-level data. As showcase, we took the DAN-KC-MBON circuitry published by Schleyer et al. [53] (Fig. 2), and extracted in close collaboration with *Drosophila* brain experts the neuron-to-neuron synaptic connectivity data from CATMAID [40]. We added these neurons as nodes to their respective compartments as child nodes (*Step 1) Preprocessing the Input Data*), and encoded the synapse count between them as connectivity.

Sagittal and transversal views can be seen in Fig. 6. In contrast to the other scenarios, we had to omit *Step 5 - Triangulation* from layouting, which is used to generate a more even distribution of nodes. The unique form of the *Drosophila* larval brain with its elongated, slim caudal extension (thoracic ganglion in green and abdominal ganglion in orange) would have been distorted otherwise. As a consequence, Fig. 6 (*No Connectivity*) shows a nice overall shape, but cluttered and overlapping nodes in the protocerebrum, especially in the optic lobe (yellow). This effect was compensated when using the distance-based *Parcellation-Derived Connectivity* (Fig. 6, *Distance*). The neighborhood-based *Parcellation-Derived Connectivity* (Fig. 6, *Neighborhood*) led to even better results for the sagittal view, as it produced a more uniform distribution in the abdominal ganglion (orange region).

Results: The result of re-imagine the showcase can be seen in Fig. 10, with the DAN-KC-MBON circuitry in the mushroom body (red), inferior protocerebrum (brown), and superior lateral protocerebrum (green). The solid arrows represent synapse count between the neurons, the dashed lines between DAN-i1 nodes (in multiple regions) indicate that it is actually the same neuron present in these three regions. The added nodes displaced adjoined regions spatially correct. According to our domain experts, this is a good first step towards representing neuron-level circuits with anatomical context. Further enhancements, e.g., adding markers for input and output locations [51], i.e., sensory input, or motor output, in combination with interactive information visualization (e.g., showing the information flow on mouse-over) could make this a valuable tool for circuit research.

Due to the differences of the data used in this study with respect to resolution (neuron vs region level) and scale (local connectivity vs whole brain connectivity) in contrast to the mouse and human, we did not perform a separate user study for this species.

6. User study

We performed a user study to investigate the effectiveness of our proposed layouting method and visual design on the perception of network visualization by domain experts. The objective was to prove the usefulness of *Spatial-Data-Driven Layouts* for brain network visualization and to receive feedback for future development. Ideally we wanted to include as many scientists as possible, to get a wide range of opinions and to be robust to individual point of views. Hence, we designed a web-based questionnaire which was sent out to scientists working with brain networks, including computer scientists, computational biologists/bioinformaticians, and neuroscientists. The full questionnaire is included in the supplementary material.

6.1. Study design

Evaluation of our approach was conducted on mouse and human brain networks. We created a web-based questionnaire to measure user performance and user experience [54] for each species separately, whereby domain expert were encouraged to participate in the studies of the species for which they felt familiar with. The order of questions was randomized to counteract a learning effect.

The studies included whole brain and partial networks in sagittal and transversal views. To compare our results, we also present visualizations with and without layouting, i.e., brain networks without our approach. Furthermore, we evaluated also the effect of the brain regions' coloring by including gray-scale images. The questionnaire consists of four parts:

- **(S1) Identifying Nodes/Connections:** The first part was to measure the efficiency of the layouting in providing orientation. Therefore, we tested the viewers by checking how fast they can find specific nodes and connections in the graph compared to graphs without *Spatial-Data-Driven Layouting*. Here, we measured the time how long it takes to click on the node with the strongest connection to a given node in a whole brain network. This task was performed on different transversal views, with and without applied *Spatial-Data-Driven Layouting*, and different regions. In this experiment, the question order was randomized to prevent unexpected learning effects.
- **(S2) Visualization of Anatomical Context:** Here, we showed whole and partial brain networks covering different parts of the brain. We varied different parameters, such as the *Shadow Node Ratio* (Section 4.2, *Step 2 - Making the Graph Anatomically Complete*) and the *Number of Background Regions* (Section 4.2, *Step 6 - Background Parcellation*), then we asked the participants to rank them by clarity, and how well they are suitable as paper figures and for educational purpose based on a Likert scale. Furthermore, we compared artistically drawn figures from neuroscientific publications [45,50] to similar figures generated with our approach.
- **(S3) Edge Visualization:** Here we experimented with different types of edge rendering. Participants were asked to rank different numbers of edges (top 10%, 20% or 30% of the edges), as well as different edge routing layouts (direct arrows, organic edge routing with varied parameters, and orthogonal edge routing, see Fig. 11), based on clarity and suitability for publications.
- **(S4) Demographic Data:** The last part includes personal questions including the current position held by the participant, level of expertise, familiarity with the brain-region ontology, color-blindness, and gender.

The major results of the user study can are shown in Table 1, and are summarized in the following subsections.

Table 1
Results of the user-study of Part (S1) Identifying nodes/connections, Part (S2) Visualization of anatomical context, Part (S3) Edge visualization, and Part (S4) demographic data.

Participants	Mouse 8 (3 female, 5 male)	Human 6 (3 female, 3 male)
Part (S1): Median task completion time		
(a) directly projected layout	31 s	43 s
(b) SDD[a] layout without background	24 s	32 s
(c) SDD[a] layout with background	30.5 s	30 s
Part (S2) Anatomical context		
preferred our approach over 2D projection on different hierarchy levels (votes)	6	5
Number of Background Regions least | middle | most (votes)	5 | 2 | 1	0 | 6 | 0
Number of *Shadow Nodes* least | most (votes)	2 | 6	1 | 5
Shadow Nodes background colored | gray (votes)	1 | 7	1 | 5
helpfulness of background scores[b]	4.05	4.58
visual appealing of re-imagined figure[b]	3.36	3.33
Part (S3) Preferred edge routing (votes)		
direct (clarity | paper | education)	3 | 3 | 3	2 | 2 | 2
organic (clarity | paper | education)	5 | 5 | 5	4 | 4 | 4
orthogonal (clarity | paper | education)	0 | 0 | 0	0 | 0 | 0
Part (S4) Demographics		
female | male	3 | 5	3 | 3
postdoc | principal investigators	5 | 3	5 | 1
neurosci. | bioinf.| comp. sci.	4 | 2 | 2	2 | 2 | 2
red-green color weakness	2	1

[a]SDD = *Spatial-Data-Driven*.
[b]1 (poor) to 5 (good).

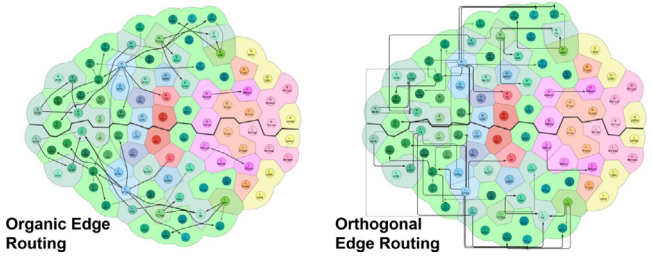

Fig. 11. Edge routing algorithms that were used in the user study in addition to direct arrows.

6.2. Results

We recruited eight participants for the mouse user study (three female and five male participants), and six participants for the human (three female and three male participants) to investigate the feasibility of the presented visualization. All participants of the human user study took also part in the mouse user study. All participants are at a senior level (postdoctoral researchers principal investigators) with domain knowledge. Six participants have worked and are familiar with the *Allen Mouse Brain Common Coordinate Framework* [36] and three with the *Allen Human Reference Atlas,Ding2016*.

Part (S1) consists of three configuration settings of a network covering structural connectivity over the whole brain, including (a) directly projected layout, (b) *Spatial-Data-Driven Layout* without background, and (c) *Spatial-Data-Driven Layout* with background. There are in total six clicking questions (for each layout, we prepared two questions) and measured the task completion time. Only one participant made a mistake which happened when the graph was synthesized directly from the projection (a). It is straightforward that the task completion time of (b) is shorter than (a), due to the few occlusions in (b). In case (c) for the mouse study, the time increased compared to (b), which may be because the colored background induced another layer of visual complexity. This was also mentioned by the participants that the concatenation of strong colors makes it difficult to read the connectivity of entities in the diagram. For the human study, the completion of (c) was as fast as (b). This might be an effect of the more spherical form of the human brain relative to the mouse brain. Here, a transversal projection leads to higher deformation of the anatomical structure due to a higher displacement of the nodes. Hence, the background context supported the spatial orientation to find nodes/connections rather than to divert the viewers focus.

In **Part (S2)**, we tested different settings for the visualization, consisting of four questions with different hierarchy levels, two questions with different levels of background detail (*Number of Background Regions*), three question with varying size of background context (*Shadow Node Ratio*) for sub-networks, and additional questions regarding coloring thereof. For the different hierarchy levels, we tested sagittal and transversal views, and the three configuration settings described in *Part (S1)*. On average, six participants considered our approach most visually preferable at coarse, middle and detailed levels, respectively. For the *Number of Background Regions*, they preferred rather low numbers to represent major brain regions.

Half of the participant preferred to read sub-networks with the most background, i.e., highest *Shadow Node Ratio*, while the two neuroscientist with color weakness preferred simple sub-network without background. In comparison to full color images, seven out of eight participants prefer the mixture of gray and color background. The helpfulness of the background for spatial orientation was considered as for the mouse brain 4.04 on a scale between 1 (poor) and 5 (good) and was considered even higher with 4.58 for the human brain.

When showing the graphs in Figs. 7 and 9, where we re-imagined a hand-crafted image from an existing work [45,50] with our approach, we received an average ranking of 3.63 (1 is poor and 5 is good) for the mouse and 3.33 for the human. The slightly lower score for human might be either due to the low number of participants (no significant difference), or because of the higher complexity in terms of node and edge count in the human figure.

In **Part (S3)**, we also did a comparison on various styles of edge rendering and various numbers of edges. Participants preferred fewer edges for clarity due to the reduction of clutter. Not surprisingly, half of the participants chose the organic edge routing,

since curve is well-known for its effectiveness of tracing a path in visualization [55].

Finally, in **Part (S4)**, we did not find demographic differences, except for the preference of neuroscientists with color weakness for sub-network visualization without background.

6.3. General feedback

We also received some general feedback from the participants. One participant indicated that "*Good work with the nice, comprehensive visualisations*". Another participant mentioned that "*the honeycomb parcellation is very nice, the edges visibility in the long-range is quite tricky*". Another participant suggests to us to "*summarize these arrows into one arrow, pointing to some meaningful position in the target hierarchy, and only then branching out to each target area separately*", i.e to bundle edges of nodes that project between two brain regions on a higher hierarchy level.

7. Discussion

Section 5 showed the potential and relevance of our approach in neurobiological research on different species. The results of the user studies in Section 6 indicate a positive effect of *Spatial-Data-Driven Layouts* (**R1**) on the perception of brain networks by neuroscientists. By reproducing the results of the user studies from mouse for human, we demonstrated a species-independence of our approach (**R2**). The following discusses the combined output of these studies in terms of usefulness of the visual design, limitations, and potential further improvements.

Visual Design. The overall approach of layouting node-link diagrams representing brain networks according to their spatial relations was perceived as intuitively by our domain experts during the user studies. Here, we showed that the task of finding nodes and connections in a graph can be performed faster when using *Spatial-Data-Driven Layouts* over simple 2D projections of 3D networks. Finding the nodes was possible by providing the graph in perspective views, which are required to grasp the orientation of the graph (**R4**).

The user studies showed that there is no unique solution to how many background brain regions (determined by the *Number of Background Regions* parameter) are ideal. The participants rather preferred either few or many (**R6**). Furthermore, the background can even interfere with edges, which resulted in diminishing task performance in the mouse user study, part (S1).

Furthermore, including brain regions, that are not part of sub-networks as *Shadow Nodes* (set by the (*Shadow Node Ratio*), was considered as highly useful, since it preserves the overall shape of the brain (**R1, R3**) and allows the user to compare different graphs. A larger *Shadow Node Ratio* was preferred, as it provides a shape similar to a network covering the whole brain. Rendering this additional context in shades of gray was chosen to not divert the viewers focus, and was favored by a majority of participants.

Limitations. In general, our approach is spatial-data-driven and does not require manual re-positioning of nodes. The only two parameters specific to our approach, *Shadow Node Ratio* and *Number of Background Regions*, are mainly influencing the anatomical context, and not the arrangement of the nodes per se. Nevertheless, the layouting is performed with force-directed algorithms, which are typically not parameter free. During the development of this method, we found that these parameters depend strongly on the type of *Parcellation-derived Connectivity* and the size of the graph. Our implementation can produce these graphs in an instant, so adapting the parameters interactively via sliders (*Supplementary Video 1*) leads to brain anatomy representing graphs (*R5*) that also retain the overall shape of the brain (*R3*). A way to investigate the parameter space automatically would be to use optimization algorithms such as gradient decent. Here, the force-directed layouting parameters could be optimized towards maximizing the *Parcellation-derived Connectivity* between neighboring nodes, i.e., what is close in the anatomical reference space is also close in the layout. Note, that the purpose of this paper was to show that *Parcellation-derived Connectivity* can be used for layouting networks while maintaining spatial organization. Hence, the optimization of parameters for force-directed layouting was not in the scope, for they represent only one exemplary way of layouting *Parcellation-derived Connectivity*. As a consequence, this approach would not guarantee keeping the overall shape of the brain.

Another limitation is that, the background parcellation depends on the availability of *Hierarchical Representation of Brain Regions*, which is not necessarily given for every species. Creating a *Parcellation-derived Connectivity* can be also seen as an overhead, that not every potential user is willing to take.

To ensure that nodes do not overlap (**R8**) and are evenly distributed, we added an additional layouting step based on triangulation between nodes (Section 4.2, *Step 5 - Triangulation*). In the *Drosophila* usage scenario, we had to omit this task because its slim, caudal extension was distorted otherwise. Therefore, we can only recommend this step for species with bulkier brains such as the mouse and the human.

Potential. Our user study showed that the figures that were re-imagined from hand-crafted paper illustrations are well perceived, so they could be considered for publications. However, more interactive features could enable this tool to be used also directly for neuroscience research. For example, features, such as highlighting the information flow from and to a node, edge filtering, interactive changing the networks hierarchy level, hierarchical edge bundling, or overlaying additional region-level data such as gene expression, might enable novel visual analytics workflows.

Furthermore, our proposed visualization of neuronal circuits in the *Drosophila* larval brain represents only a first step. Further developing the visualization to include markers for input/output locations, or a different encoding for neurons that span multiple brain regions, could make this approach a valuable addition to currently used circuit diagrams.

Last but not least, we want to point out that our approach is not limited to spatial brain networks. In principle, one could use this approach to "flatten" spatial 3D networks from different disciplines to 2D graphs. Even without a hierarchical representation of regions, and consequently without the rendering of context in the background, nodes can still be layouted according to their spatial relations, and therefore provide spatial orientation.

8. Conclusion

In this paper, we present a novel approach to visualize brain networks via spatial-data-driven layouting, and a visual design to render anatomical context. Our method is data-driven, so it does not require the manual definition of spatial restrictions to generate anatomically feasible layouts, independent of species or perspective. This is enabled by using *Parcellation-derived Connectivity*, generated from brain atlases, to perform graph layouting with standard force-directed algorithms.

We show in several case-studies on different species, that this results in a positioning of nodes that inherently represent the spatial relations between brain regions, i.e., brain regions that are adjoined in the reference space are close together in the graph. This indicates that our method could be applied to various species; generating novel anatomical layouts of neuroscientific networks. In further research, one could even investigate the

generalization of this approach by applying it to other disciplines, where "flattening" a 3D network to a 2D space would be beneficial.

To provide further guidance, we developed a visual design to highlight the networks anatomical context. Here, we added a color-coded parcellation to the background of a brain network, to indicate major anatomical regions, and provide an overall shape, independent of the graph's completeness. This background is adaptable with regards to anatomical detail, to represent either anatomical size or the number of connections.

We evaluated both the layouting and the design in a web-based user study with domain experts from the field of neuroscience, computer science, bioinformatics, and computation biology, which showed the general applicability of our approach for neuroscientific visualization. This suggest, that *Spatial-Data-Driven Layouts* are valuable, not only to domain experts working with the data, but also to their audience, to give an understanding of brain networks that would be otherwise hard to grasp.

For the future, we plan to integrate this approach into an interactive visual analytics tool to enable neuroscientists a quick deployment to their data, and ad hoc adjustment regarding the method's parameters and brain regions of interest, to make this approach available to a wider audience. Furthermore, we want to enhance the neuron-level visualization and visual design of the *Drosophila* larval network graphs for a more detailed circuit representation.

CRediT authorship contribution statement

Florian Ganglberger: Conceived the method, Designed the user study, Analyzed the results, Wrote the manuscript. **Monika Wißmann:** Conceived the method, Implemented the method, Designed the user study, Wrote the manuscript. **Hsiang-Yun Wu:** Designed and implemented the user study, Analyzed the results, Wrote the manuscript. **Nicolas Swoboda:** Generated the Drosophila usage scenario figure. **Andreas Thum:** Helped to shape requirements, Provided data and use cases. **Wulf Haubensak:** Helped to shape requirements, Provided data and use cases. **Katja Bühler:** Conceived the method, Wrote the manuscript.

Declaration of competing interest

The authors declare that they have no known competing financial interests or personal relationships that could have appeared to influence the work reported in this paper.

Acknowledgments

This research was funded in part by the Austrian Science Fund (FWF) I 4836-B. For the purpose of open access, the author has applied a CC BY public copyright license to any Author Accepted Manuscript version arising from this submission.

VRVis is funded by BMVIT, BMDW, Styria, SFG and Vienna Business Agency in the scope of COMET–Competence Centers for Excellent Technologies (854174) which is managed by FFG. We want to thank Gwendolyn Rippberger for a first prototype predating Monika Wißmanns implementation. Furthermore, we want to thank the participants of the user study, especially the Haubensak group at the Institute of Molecular Pathology in Vienna and Böhringer-Ingelheim in Biberach an der Riß. Last but not least we want to thank Thomas Torsney-Weir for writing support.

Appendix A. Supplementary data

Supplementary material related to this article can be found online at https://doi.org/10.1016/j.cag.2022.04.014.

References

[1] Margulies DS, Böttger J, Watanabe A, Gorgolewski KJ. Visualizing the human connectome. NeuroImage 2013;80:445–61. http://dx.doi.org/10.1016/j.neuroimage.2013.04.111.

[2] Strauch M, Hartenstein V, Andrade IV, Cardona A, Merhof D. Annotated dendrograms for neurons from the larval fruit fly brain. In: VCBM 2018 - Eurographics workshop on visual computing for biology and medicine. 2018, http://dx.doi.org/10.2312/vcbm.20181229.

[3] Sporns O. Structure and function of complex brain networks. Dialogues Clin Neurosci 2013;15(3):247–62. http://dx.doi.org/10.31887/DCNS.2013.15.3/osporns.

[4] Larson SD, Martone ME. Ontologies for neuroscience: What are they and what are they good for? Front Neurosci 2009;3(1):60–7. http://dx.doi.org/10.3389/neuro.01.007.2009.

[5] Marai GE, Pinaud B, Bühler K, Lex A, Morris JH. Ten simple rules to create biological network figures for communication. PLoS Comput Biol 2019;15(9). http://dx.doi.org/10.1371/journal.pcbi.1007244.

[6] Salvador R, Suckling J, Coleman MR, Pickard JD, Menon D, Bullmore E. Neurophysiological architecture of functional magnetic resonance images of human brain. Cerebral Cortex 2005;15(9):1332–42. http://dx.doi.org/10.1093/cercor/bhi016.

[7] Ganglberger F, Swoboda N, Frauenstein L, Kaczanowska J, Haubensak W, Bühler K. BrainTrawler: A visual analytics framework for iterative exploration of heterogeneous big brain data. Comput Graph 2019;82:304–20. http://dx.doi.org/10.1016/j.cag.2019.05.032.

[8] Xia M, Wang J, He Y. BrainNet viewer: a network visualization tool for human brain connectomics. PLoS One 2013;8(7). http://dx.doi.org/10.1371/journal.pone.0068910.

[9] Sorger J, Bühler K, Schulze F, Liu T, Dickson B. NeuroMAP—Interactive graph-visualization of the fruit fly's neural circuit. In: 2013 IEEE symposium on biological data visualization. IEEE; 2013, p. 73–80. http://dx.doi.org/10.1109/BioVis.2013.6664349.

[10] Schöttler S, Yang Y, Pfister H, Bach B. Visualizing and interacting with geospatial networks: A survey and design space. Comput Graph Forum 2021;40(6):5–33. http://dx.doi.org/10.1111/cgf.14198.

[11] ten Caat M, Maurits NM, Roerdink JB. Data-driven visualization and group analysis of multichannel EEG coherence with functional units. IEEE Trans Vis Comput Graphics 2008;14(4):756–71. http://dx.doi.org/10.1109/TVCG.2008.21.

[12] Gerhard S, Daducci A, Lemkaddem A, Meuli R, Thiran J-P, Hagmann P. The connectome viewer toolkit: An open source framework to manage, analyze, and visualize connectomes. Front Neuroinf 2011;5:3. http://dx.doi.org/10.3389/fninf.2011.00003.

[13] Ribeiro AS, Lacerda LM, Ferreira HA. Multimodal imaging brain connectivity analysis (MIBCA) toolbox. PeerJ 2015;3:e1078. http://dx.doi.org/10.7717/peerj.1078.

[14] Rubinov M, Sporns O. Complex network measures of brain connectivity: Uses and interpretations. NeuroImage 2010;52(3):1059–69. http://dx.doi.org/10.1016/j.neuroimage.2009.10.003.

[15] Bassett DS, Sporns O. Nature neuroscience. 2017, http://dx.doi.org/10.1038/nn.4502, arXiv:0106096v1.

[16] Richiardi J, Altmann A. Correlated gene expression supports synchronous activity in brain networks. Science 2015;348(6240):11–4. http://dx.doi.org/10.1126/science.1255905.

[17] Zalesky A, Fornito A, Bullmore ET. Network-based statistic: Identifying differences in brain network. NeuroImage (4):1197–207.

[18] LaPlante RA, Douw L, Tang W, Stufflebeam SM. The connectome visualization utility: Software for visualization of human brain networks. PLoS One 2014;9(12):e113838. http://dx.doi.org/10.1371/journal.pone.0113838.

[19] Irimia A, Chambers MC, Torgerson CM, Filippou M, Hovda DA, Alger JR, et al. Patient-tailored connectomics visualization for the assessment of white matter atrophy in traumatic brain injury. Front Neurol 2012;3:10. http://dx.doi.org/10.3389/fneur.2012.00010.

[20] Bezgin G, Reid AT, Schubert D, Kötter R. Matching spatial with ontological brain regions using java tools for visualization, database access, and integrated data analysis. Neuroinformatics 2009;7(1):7–22.

[21] Beyer J, Al-Awami A, Kasthuri N, Lichtman JW, Pfister H, Hadwiger M. ConnectomeExplorer: Query-guided visual analysis of large volumetric neuroscience data. IEEE Trans Vis Comput Graphics 2013;19(12):2868–77. http://dx.doi.org/10.1109/TVCG.2013.142.

[22] Beyer J, Hadwiger M, Al-Awami A, Jeong W-K, Kasthuri N, Lichtman JW, et al. Exploring the connectome: Petascale volume visualization of microscopy data streams. IEEE Comput Graph Appl 2013;33(4):50–61. http://dx.doi.org/10.1109/MCG.2013.55.

[23] Alper B, Bach B, Henry Riche N, Isenberg T, Fekete J-D. Weighted graph comparison techniques for brain connectivity analysis. In: Proceedings of the SIGCHI conference on human factors in computing systems. CHI '13, New York, NY, USA: ACM; 2013, p. 483–92. http://dx.doi.org/10.1145/2470654.2470724.

[24] Poldrack RA, Laumann TO, Koyejo O, Gregory B, Hover A, Chen M-Y, et al. Long-term neural and physiological phenotyping of a single human. Nature Commun 2015;6:8885.
[25] Murugesan S, Bouchard K, Brown JA, Hamann B, Seeley WW, Trujillo A, et al. Brain modulyzer: interactive visual analysis of functional brain connectivity. IEEE/ACM Trans Comput Biol Bioinform 2016;14(4):805–18.
[26] Conte G, Ye AQ, Almryde KR, Ajilore O, Leow AD, Forbes AG. Intrinsic geometry visualization for the interactive analysis of brain connectivity patterns. In: Visualization and data analysis. 2016.
[27] Conte G, Ye AQ, Forbes AG, Ajilore O, Leow A. BRAINtrinsic: A virtual reality-compatible tool for exploring intrinsic topologies of the human brain connectome. In: Brain informatics and health. Springer; 2015, p. 67–76. http://dx.doi.org/10.1007/978-3-319-23344-4_7.
[28] Keiriz JJG, Zhan L, Ajilore O, Leow AD, Forbes AG. NeuroCave: A web-based immersive visualization platform for exploring connectome datasets. Netw Neurosci 2018;2(3):344–61. http://dx.doi.org/10.1162/netn_a_00044.
[29] Jianu R, Demiralp C, Laidlaw DH. Exploring brain connectivity with two-dimensional neural maps. IEEE Trans Vis Comput Graphics 2012;18(6):978–87. http://dx.doi.org/10.1109/TVCG.2011.82.
[30] McGraw T. Graph-based visualization of neuronal connectivity using matrix block partitioning and edge bundling. In: International Symposium on Visual Computing. Springer; 2015, p. 3–13. http://dx.doi.org/10.1007/978-3-319-27857-5_1.
[31] Eades P, Lai W, Misue K, Sugiyama K. Layout adjustment and the mental map. J Vis Lang Comput 1995;6(2):183–210.
[32] Holten D, Van Wijk JJ. Force-directed edge bundling for graph visualization. In: Comput Graph Forum. 28, (3):Wiley Online Library; 2009, p. 983–90. http://dx.doi.org/10.1111/j.1467-8659.2009.01450.x.
[33] Böttger J, Schäfer A, Lohmann G, Villringer A, Margulies DS. Three-dimensional mean-shift edge bundling for the visualization of functional connectivity in the brain. IEEE Trans Vis Comput Graphics 2014;20(3):471–80. http://dx.doi.org/10.1109/TVCG.2013.114.
[34] Ji C, Maurits NM, Roerdink JBTM. Data-driven visualization of multichannel EEG coherence networks based on community structure analysis. Appl Netw Sci 2018;3(1):41. http://dx.doi.org/10.1007/s41109-018-0096-x.
[35] Wu H-Y, Nollenburg M, Viola I. Multi-level area balancing of clustered graphs. IEEE Trans Vis Comput Graphics 2020;1. http://dx.doi.org/10.1109/TVCG.2020.3038154.
[36] Wang Q, Ding SL, Li Y, Royall J, Feng D, Lesnar P, et al. The Allen Mouse Brain common coordinate framework: A 3D reference atlas. Cell 2020;181(4):936–53. http://dx.doi.org/10.1016/j.cell.2020.04.007.
[37] Larvalbrain. 2021, http://www.larvalbrain.org/. [Accessed 08 November 2021].
[38] Van Essen DC, Smith SM, Barch DM, Behrens TE, Yacoub E, Ugurbil K. The WU-Minn human connectome project: An overview. NeuroImage 2013;80:62–79. http://dx.doi.org/10.1016/j.neuroimage.2013.05.041.
[39] Oh SW, Harris JA, Ng L, Winslow B, Cain N, Mihalas S, et al. A mesoscale connectome of the mouse brain. Nature 2014;508(7495):207–14. http://dx.doi.org/10.1038/nature13186.
[40] Saalfeld S, Cardona A, Hartenstein V, Tomančák P. CATMAID: Collaborative annotation toolkit for massive amounts of image data. Bioinformatics 2009;25(15):1984–6. http://dx.doi.org/10.1093/bioinformatics/btp266.
[41] Dogrusoz U, Giral E, Cetintas A, Civril A, Demir E. A layout algorithm for undirected compound graphs. Inform Sci 2009;179(7):980–94. http://dx.doi.org/10.1016/j.ins.2008.11.017.
[42] Ding SL, Royall JJ, Sunkin SM, Ng L, Facer BA, Lesnar P, et al. Comprehensive cellular-resolution atlas of the adult human brain. J Comp Neurol 2016;524(16):3127–608. http://dx.doi.org/10.1002/cne.24080.
[43] Cytoscape.js - A graph theory (network) library for visualisation and analysis. 2021, https://js.cytoscape.org/. [Accessed 08 November 2021].
[44] Feng D, Lau C, Ng L, Li Y, Kuan L, Sunkin SM, et al. Exploration and visualization of connectivity in the adult mouse brain. Methods 2015;73:90–7. http://dx.doi.org/10.1016/j.ymeth.2015.01.009.
[45] Russo SJ, Nestler EJ. The brain reward circuitry in mood disorders. Nat Rev Neurosci 2013;14(9):609–25. http://dx.doi.org/10.1038/nrn3381.
[46] Interactive Atlas viewer. 2021, http://atlas.brain-map.org/. [Accessed 26 March 2021].
[47] Hawrylycz MJ, Lein ES, Guillozet-Bongaarts AL, Shen EH, Ng L, Miller JA, et al. An anatomically comprehensive atlas of the adult human brain transcriptome. Nature 2012;489(7416):391–400. http://dx.doi.org/10.1038/nature11405.
[48] Ding S-L, Royall JJ, Sunkin SM, Facer BA, Lesnar P, Bernard A, et al. Allen human reference Atlas – 3D, 2020. 2020, RRID:SCR_017764.
[49] Amunts K, Mohlberg H, Bludau S, Zilles K. Julich-Brain: A 3D probabilistic Atlas of the human brain's cytoarchitecture. Science 2020;369(6506):988–92. http://dx.doi.org/10.1126/science.abb4588.
[50] Gotter AL, Webber AL, Coleman PJ, Renger JJ, Winrow Dr. CJ. International union of basic and clinical pharmacology. LXXXVI. orexin receptor function, nomenclature and pharmacology. Pharmacol Rev 2012;64(3):389–420. http://dx.doi.org/10.1124/pr.111.005546.
[51] Saumweber T, Rohwedder A, Schleyer M, Eichler K, Chen YC, Aso Y, et al. Functional architecture of reward learning in mushroom body extrinsic neurons of larval drosophila. Nature Commun 2018;9(1):1104. http://dx.doi.org/10.1038/s41467-018-03130-1.
[52] Hartenstein V, Younossi-Hartenstein A, Lovick JK, Kong A, Omoto JJ, Ngo KT, et al. Lineage-associated tracts defining the anatomy of the Drosophila first instar larval brain. Dev Biol 2015;406(1):14–39. http://dx.doi.org/10.1016/j.ydbio.2015.06.021.
[53] Schleyer M, Weiglein A, Thoener J, Strauch M, Hartenstein V, Weigelt MK, et al. Identification of dopaminergic neurons that can both establish associative memory and acutely terminate its behavioral expression. J Neurosci 2020;40(31):5990–6006. http://dx.doi.org/10.1523/JNEUROSCI.0290-20.2020.
[54] Isenberg T, Isenberg P, Chen JJ, Sedlmair M, Möller T. A systematic review on the practice of evaluating visualization. IEEE Trans Vis Comput Graphics 2013;19:2818–27. http://dx.doi.org/10.1109/TVCG.2013.126.
[55] Wu H-Y, Niedermann B, Takahashi S, Roberts MJ, Nöllenburg M. A survey on transit map layout from design, machine, and human perspectives. Comput Graph Forum (Special Issue of EuroVis 2020) 2020;39(3). http://dx.doi.org/10.1111/cgf.14030.